

ORBITS AND STRUCTURE OF QUADRUPLE SYSTEMS GJ 225.1 AND FIN 332

A. TOKOVININ

Cerro Tololo Inter-American Observatory — NSF's NOIRlab, Casilla 603, La Serena, Chile
Draft version August 7, 2020

ABSTRACT

Only a handful of quadruple systems with two accurate inner visual orbits are known. Architecture of two such systems is studied here to determine period ratios, mutual orbit orientation, and other parameters; updated orbital elements and their errors are derived. Gliese 225.1 (HIP 28442) is composed of three K-type and one M-type dwarfs and has inner orbital periods of 67.2 ± 0.2 and 23.4 ± 0.5 yr. Its inner orbits have small mutual inclination and are likely coplanar with the outer orbit of ~ 2 kyr period. The quadruple system FIN 332 (HIP 92037) consists of four early A type stars with similar masses and magnitudes. Both its inner orbits with periods of 27.6 ± 0.2 and 39.8 ± 0.4 yr have large eccentricities (0.82 and 0.84). Their orientation in the sky is remarkably similar. In contrast, the outer orbit with a period of ~ 5 kyr has a large relative inclination to the inner orbits. Dynamics and formation of these quadruple systems are briefly discussed.

Accepted for publication in Astronomy Letters.

Keywords:

1. INTRODUCTION

Architecture of hierarchical stellar systems bears traces of their formation mechanisms, still not fully understood. Systems of 2+2 hierarchy considered here (two close pairs on a wide orbit around each other) are rather typical. Multiplicity statistics in the solar neighborhood shows that the incidence of inner subsystems in two components of a wide binary is correlated rather than independent, hinting that stars in 2+2 quadruples formed together (Tokovinin 2014). Furthermore, known 2+2 quadruples show some correlation between their inner periods and often have all four components of similar masses (Tokovinin 2008). However, it is not clear whether 2+2 quadruples formed preferentially outside-in by successive fragmentation of gas at large, then small scales, inside-out (inner subsystems formed first and later became bound later), or in a common event like cloud collision (Whitworth 2001).

Recently, Zasche et al. (2019) studied a large sample of 2+2 quadruple systems where both inner pairs are eclipsing (doubly eclipsing). In these systems, both close inner binaries have large inclinations, suggesting (but not proving) coplanarity of their orbits. Even more surprisingly, the ratio of the inner periods was found to have preferential values around 1 and 1.5 and to avoid values around 2, implying some kind of a resonance between inner orbits. Considering short inner periods and the likely large outer periods, existence of dynamical interactions between inner orbits leading to a resonance appeared challenging. Tremaine (2020) has picked up the challenge and determined conditions where such resonances can occur. Significant migration of inner binaries to shorter periods and their moderate separation seem to be necessary to explain the resonances found by Zasche et al.

These discoveries prompted me to look at wider 2+2 quadruples where both inner subsystems have known vi-

sual orbits. Apart from the period ratio, mutual orientation of inner orbits and other parameters contain information that can throw some light on the formation mechanisms. A prototype of such quadruples is ϵ Lyr containing four similar A-type stars. However, the long periods of its inner subsystems (1800 and 724 yr) do not allow calculation of accurate orbits, owing to the lack of sufficient coverage. Situations where both inner visual orbits in a 2+2 quadruple can be accurately constrained by observations are rare; only about a dozen of such cases are known. Two 2+2 quadruples with accurate inner orbits are featured here, GJ 225.1 and FIN 332. Their known orbits are re-accessed and updated using recent observations, and the properties of the stars are determined taking advantage of Gaia parallaxes (Gaia collaboration 2018).

2. GLIESE 225.1

A classical visual triple system HJ 3823 AB and AB,C (WDS J06003–3102, HIP 28442, HD 40887, GJ 225.1) turned into a 2+2 quadruple when a faint satellite near star C was discovered in 2004 by Tokovinin et al. (2005) using adaptive-optics imaging in the infra-red (IR). The 23-yr period of this new subsystem C,E was initially found from astrometric perturbations (wobble) in the motion of the outer binary AB,C. Now, 15 years later, the orbit of C,E is well covered by speckle interferometry at the Southern Astrophysical Research (SOAR) telescope (Tokovinin et al. 2020, and references therein), allowing calculation of accurate orbital elements. The orbit of A,B, already well established from historic micrometer measurements, also benefits from accurate modern speckle astrometry.

The Gaia data release 2 (Gaia collaboration 2018) provides astrometry of A and C as though they were single stars. The separation of A,B in 2015.5 was $0''.58$, and the Gaia astrometry of this unresolved pair has large errors, e.g. parallax 53.97 ± 0.42 mas. The star C was also unresolved by Gaia, but the magnitude difference of C,E is

Table 1
Orbital elements

System	P yr	T yr	e	a "	Ω °	ω °	i °	ΣM M_{\odot}	$K_1 + K_2$ km s ⁻¹
GJ 225.1 A,B	67.22 ±0.19	1998.08 ±0.21	0.462 ±0.018	0.953 ±0.017	126.2 ±0.2	282.9 ±0.4	101.9 ±0.3	1.14 ±0.01	6.1 ...
GJ 225.1 C,E	23.38 ±0.54	2015.44 ±0.13	0.216 ±0.013	0.433 ±0.007	146.8 ±0.2	178.6 ±2.2	98.4 ±0.2	0.90 ±0.01	10.9 ...
GJ 225.1 AB,CE	2100	1934.0	0.200	11.40	147.6	85.1	100.2	2.06	3.0
FIN 332 Aa,Ab	27.62 ±0.16	1994.00 ±0.23	0.820 ±0.012	0.0911 ±0.0009	136.0 ±1.2	4.6 ±4.1	107.9 ±1.2	4.66 ±0.14	5.2 ...
FIN 332 Ba,Bb	39.76 ±0.37	2005.09 ±0.33	0.843 ±0.020	0.120 ±0.008	119.3 ±1.5	305.9 ±4.1	106.9 ±1.6	5.1 ±1.0	3.9 ...
STF 2375 A,B	5000	557	0.5	3.64	167.5	143.4	64.5	8.9	...

large, the motion in 2015.5 was slow (it was near maximum elongation), hence the Gaia astrometry of C is more reliable. The parallax of C, 54.82 ± 0.08 mas, is adopted as the distance to the system (18.24 pc, distance modulus 1.30 mag).

2.1. Orbits of GJ 225.1

Table 1 gives updated orbits of the two inner subsystems A,B and C,E of GJ 225.1 and the tentative outer orbit of AB,CE. The elements and their errors are determined by weighted least-squares fit, where weights are inversely proportional to the squares of adopted measurement errors (Tokovinin 2016). The errors are confirmed by fitting many artificially perturbed data sets. This procedure also gives the relative error of the quantity a^3/P^2 that determines the mass sum, accounting for the correlation between a and P .

The inner orbits are plotted in Figures 1 and 2. All orbits are retrograde (with clockwise rotation) and have a similar orientation. The last two columns of Table 1 give the mass sum computed with the parallax of 54.82 mas and the full radial velocity (RV) amplitude $K_1 + K_2$ derived from the orbital elements and the masses estimated below. The a^3/P^2 ratio is measured with the relative error of 0.056 and 0.007 for A,B and C,E, respectively; the full visual coverage of the A,B orbit gives less information on the mass than the still incomplete but more accurate coverage of C,E. The error of the Gaia parallax contributes a relative error of the mass sum of 0.0044. The mass sums are $1.16 \pm 0.06 M_{\odot}$ for A,B and $0.900 \pm 0.008 M_{\odot}$ for C,E. The resulting mass sum of the whole system is $2.06 M_{\odot}$.

The outer pair AB,CE has turned by 129.2° from 1850 to 2015.5 (Figure 2); the last position is provided by Gaia. Accurate relative positions are measured only after 2004, the rest are less accurate micrometer measurements obtained from the Washington Double Star (WDS) database (Mason et al. 2001). The motion is almost rectilinear, and the outer orbit is not constrained well enough. The 391-yr orbit of AB,C computed by Baize (1980) is not viable. I fixed the eccentricity, fitted all elements, and refined the orbit further by fixing the period and semimajor axis to values that assure the correct outer mass sum of $2.06 M_{\odot}$. The outer orbit given in Table 1 is therefore a subjective choice among many potential orbits that match the short observed arc, and for this reason no errors are provided. This orbit is needed mostly as a reference for the measurement of the inner mass ratios.

Some measurements of the outer pair refer to A,C, and some to AB,C (i.e. to the photo-center of the unresolved pair A,B). These positions are affected by orbital motions in both subsystems, and the resulting wobble contains information on the inner mass ratios. The wobble amplitude is proportional to the inner orbit semi-major axis with a scaling factor $f = q/(1+q)$ in the case of resolved measurements of A,C. The photo-center wobble has a smaller amplitude with the scaling factor $f_{\alpha} = f - r/(1+r)$, where r is the light ratio in the inner pair.

In an effort to measure the mass ratios, I subtracted the small wobble caused by the subsystem C,E from the outer positions and determined the wobble amplitude produced only by the subsystem A,B (the wavy line in Fig. 2). The result is $f_{A,B} = 0.47 \pm 0.02$, corresponding to $q_{A,B} = 0.89$. This mass ratio slightly disagrees with the relative photometry of A,B, which suggests $q_{A,B} = 0.84$, the value adopted here. The resulting wobble factor $f_{A,B} = q_{A,B}/(1+q_{A,B}) = 0.45$ is still compatible with the measured one.

The procedure was repeated by subtracting the wobble of A,B to determine the mass ratio in C,E. Given the faintness of E, $f \approx f_{\alpha}$ for this subsystem. The result is $f_{C,E} = 0.24 \pm 0.04$, hence $q_{C,E} = 0.32$. Using the mass ratios and the measured mass sums, masses of all four components are computed (Table 2). The relative motion between AB and CE measured by Gaia was compared to the motion expected from all three orbits. The agreement is not as good as might be expected, probably because the Gaia astrometry of A is seriously biased by the unresolved subsystem. Regretfully, the Gaia astrometry does not help to constrain the outer orbit.

Tokovinin et al. (2015b) measured in 2008.86 the RVs of unresolved components AB and CE, both equal to 106.5 km s^{-1} . However, the RV amplitudes in both inner orbits are much larger than the measurement error of $\sim 0.5 \text{ km s}^{-1}$, so this result does not refer to the relative RV of the centers-of-mass. The spectra of AB have a slightly asymmetric line profile, suggesting that the RV of the brighter component A was larger than the RV of B (the predicted RV difference was 5.7 km s^{-1}). This means that the orbital element $\omega_{A,B}$ in Table 1 refers to the ascending node of A. Unfortunately, the true ascending node of C,E remains unknown. It could be easily established by RV monitoring of C for several years because the RV amplitude of C is 2.5 km s^{-1} . Spectroscopic orbit of C,E would also provide accurate measurement of the mass of E.

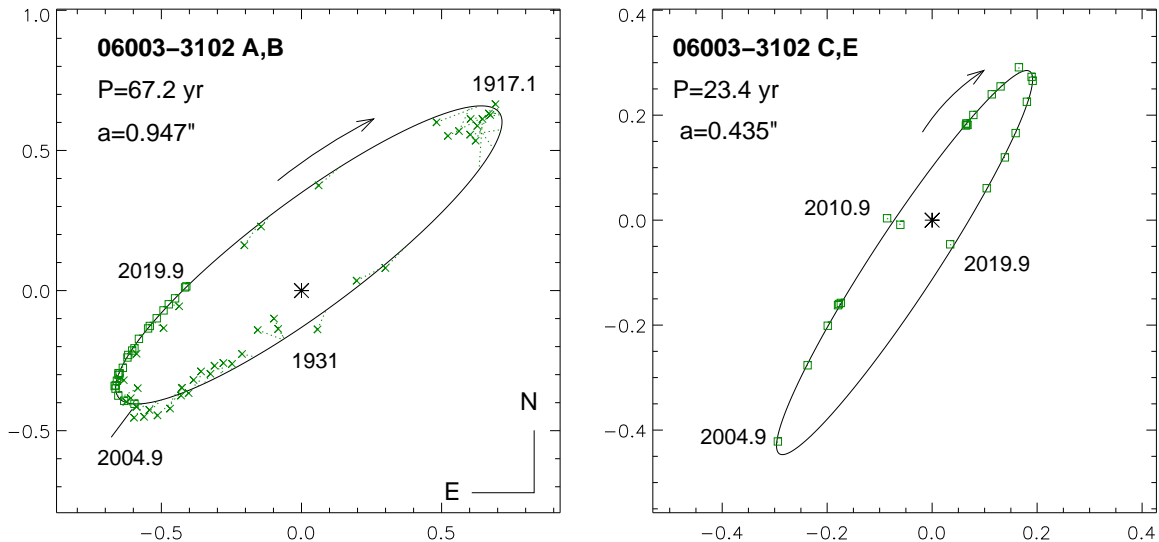


Figure 1. Orbits of the inner subsystems of GJ 225.1. In this and following Figures, the primary component of a pair is placed at the coordinate origin. The ellipse shows the orbit, with scale in arcseconds. Accurate speckle measurements are plotted by squares and connected to the respective positions on the orbit by dotted line. Less accurate data (mostly historic micrometer measurements) are plotted by crosses.

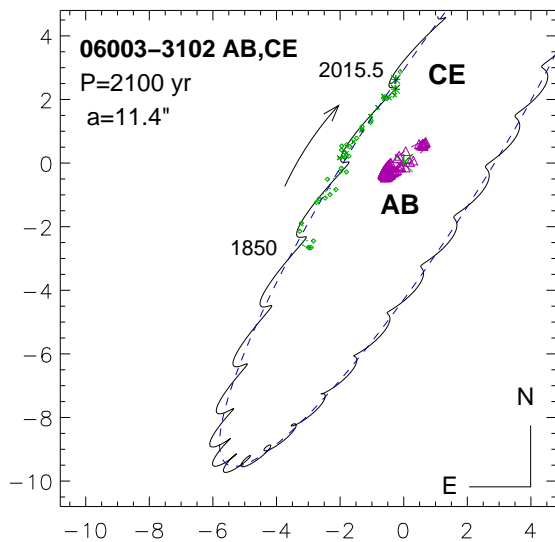


Figure 2. Tentative orbit of GJ 225.1 AB,CE. The wobble caused by the C,E subsystem is subtracted. The wavy line is the motion of C relative to A, subject to the wobble caused by the inner orbit of A,B (plotted on the same scale at the center). The dashed line is the center-of-mass motion without wobble.

As the true ascending node of the C,E orbit is not identified, the mutual inclination Φ between orbits of A,B and C,E (i.e. the angle between the vectors of orbital angular momenta) can take two values, 20.6° or 149.8° . Small inclination corresponding to co-rotation appears more likely. Inclinations of the inner orbits to the uncertain outer orbit are 20.4° and 2.0° for A,B and C,E, respectively; alternative inclinations are 151.2° and 149.8° . It seems that all three orbits are oriented approximately in one plane. Mutual inclinations exceeding 39° produce Kozai-Lidov cycles that modulate both inclination and inner eccentricity (Naoz 2016). Moderate inner eccentricities support the near-coplanarity between outer and inner orbits in this system.

Although at present the separation between AB and

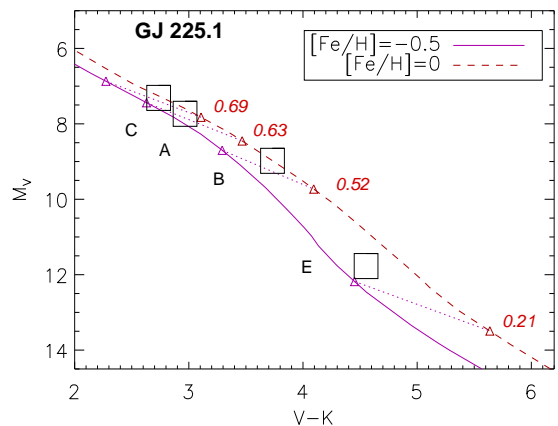


Figure 3. Location of the components of GJ 225.1 on the color-magnitude diagram. The lines are PARSEC isochrones (Bressan et al. 2012) for 1 Gyr and two metallicities values. Small triangles connected by dotted lines mark measured masses of the components (numbers in italics) on both isochrones. The components C, A, B, E (from top down) are plotted by squares.

Table 2
Components of GJ 225.1

Parameter	A	B	C	E
V (mag)	9.04	10.29	8.62	13.08
$V - K$ (mag)	2.97	3.73	2.73	4.55
\mathcal{M} (\mathcal{M}_\odot)	0.63	0.52	0.69	0.21

CE is comparable to the size of the inner orbits, hinting on possible dynamical interaction or even an instability, the observed relative motion of the wide pair suggests minimum separation at periastron of $a(1 - e) = 9''$, well above the instability limit of $\sim 3''$ according to the stability criterion by Mardling & Aarseth (2001). This hierarchical system is apparently not young and dynamically stable. The ratio of the two inner periods is 2.87 ± 0.07 .

2.2. Photometry and masses of GJ 225.1

Table 3
Components of FIN 332

Parameter	Aa	Ab	Ba	Bb
V (mag)	6.98	7.38	7.47	7.47
\mathcal{M} (\mathcal{M}_\odot)	2.46	2.20	2.14	2.14

The magnitudes of individual components in the IR bands from J to L are measured by Tokovinin et al. (2005) from the resolved images. Gaia measured the combined V magnitudes of AB and CE as 8.74 and 8.60 mag, respectively (CE is slightly brighter). The relative photometry at SOAR in the y band gives the magnitude differences of 1.25 and 4.46 mag with the rms scatter of 0.16 and 0.07 mag for A,B and C,E, respectively. Assuming $\Delta y = \Delta V$, the V magnitudes of the four stars are calculated and listed in Table 2 together with their $V-K$ colors. Star C is the most massive and the brightest of all four.

Figure 3 compares location of the components on the color-magnitude diagram (CMD) with the isochrones from Bressan et al. (2012). These dwarf stars are not evolved. The components C, A, and B are consistent with normal dwarfs of measured masses and a slightly sub-solar metallicity, $[\text{Fe}/\text{H}] \approx -0.25$ dex. The least massive star E appears somewhat brighter and bluer than expected. The discrepancy is probably explained by imperfect isochrones for such low-mass stars. The anomalously blue $J-K$ color index of E was noted by Tokovinin et al. (2005).

The fast proper motion (PM) and the large RV mean that this system belongs to the thick disk Galactic population. Considering all orbits, the PM of the system’s center-of-mass should be $(-461.8, +415.9)$ mas/yr. Together with the parallax and RV, this leads to the heliocentric velocity of $(U, V, W) = (-86.5, -47.2, -67.3)$ km s $^{-1}$.

3. FINSEN 332

The second resolved visual quadruple system considered here is known as WDS J18455+0530, ADS 11640, or FIN 332. Other identifiers are HIP 92027, HD 173495, HR 7048. The outer 2.5'' pair A,B (STF 2375AB), discovered by W. Struve in 1825, consists of two similar A1V stars, each of them itself being a close binary. W. Finsen discovered the subsystems in 1953 using an eyepiece interferometer and called them “Tweedledum and Tweedledee” because of their similarity. Rich and at times controversial observational history of the “Tweedles” is related by Mason et al. (2010). Ironically, SIMBAD does not list this pivotal paper among references on this object.

The Gaia parallaxes are 4.69 ± 0.47 mas for A and 5.48 ± 0.30 mas for B (Gaia collaboration 2018). Both are inaccurate, considering the binary nature of the sources. I adopt the dynamical parallax of 6.0 mas in the following. Individual magnitudes in Table 3 are derived from the V magnitudes of A and B measured by Gaia (6.41 and 6.72 mag) and the Δy of the close pairs measured at SOAR, 0.4 and 0.0 mag for Aa,Ab and Ba,Bb, respectively. Gaia measured the effective temperature of A and B as 9613 and 9169 K, corresponding to spectral types A0V and A1V. Masses derived from the absolute magnitudes (assuming no extinction), from 2.14 \mathcal{M}_\odot for Ba and Bb to 2.46 \mathcal{M}_\odot for Aa, match masses expected for

these spectral types. The combined color of all 4 stars $V-K = 0.17$ mag corresponds to the spectral type A2, while the actual spectral types imply $V-K \sim 0.1$ mag. Hence the interstellar extinction is indeed negligible.

3.1. Orbits of FIN 332

Mason et al. (2010) determined the first reliable orbits of subsystems Aa,Ab and Ba,Bb (periods of 27.02 and 38.6 yr, respectively) after critical evaluation and correction of the existing data. They based orbits only on speckle interferometry and ignored historic visual measurements, as well as interferometric measurements made by the author at the 1-m telescope (e.g. Tokovinin 1982). Since then, additional measurements at the 6-m telescope were published by Balega et al. (2013), and the system was monitored at SOAR. Mason (2018) updated the orbits to periods of 27.74 and 39.92 yr. The orbits listed here in Table 1 and shown in Figure 4 are very similar to those of Mason (2018). However, no errors are quoted by Mason, hence the need to re-compute the orbits here.

In fitting the orbits, small errors of 2 mas (hence high weight) are adopted for speckle measurements at SOAR and at the 6-m telescope. Other speckle data from 4-m telescopes are assigned errors of 5 mas, the measurements from smaller telescopes have larger errors. Interferometric measurements by W. Finsen are used with a low weight (30 mas error) for better definition of orbital periods, while the micrometer data are ignored. The time base of 65.7 yr (from 1953.7 to 2019.4) covers 2.4 orbital periods of Aa,Ab and 1.7 periods of Ba,Bb. The SOAR measurement of Ba,Bb in 2009.26 is added (originally published as unresolved) and the measurement in 2008.55 is reprocessed. The weighted rms residuals are 3 mas for Aa,Ab and 2 mas for Ba,Bb. Note that, despite similar input data, the semimajor axis of Ba,Bb is determined with a 10 \times larger error, compared to Aa,Ab. This is because the elements T, e, a, ω, i of Ba,Bb have large mutual correlations. Little can be done to improve the orbit because Ba,Bb is now far from the periastron. Its periastron in 2005 has not been covered, and the next one will be in 2045. On the other hand, Aa,Ab is now closing down (next periastron in 2021.6), and its regular monitoring will soon further constrain the orbit.

The estimated masses and the orbit of Aa,Ab yield the dynamical parallax of 6.0 mas, while the less certain orbit of Ba,Bb corresponds to the dynamical parallax of 6.4 mas. If the element ω of Ba,Bb is fixed at 310 $^\circ$ (only one standard deviation off the best fit), the semimajor axis of Ba,Bb increases to 0.113'' and the dynamical parallax becomes 6.0 mas. Forcing ω does not affect the period. The ratio of inner periods in this quadruple system is 1.44 ± 0.02 .

The outer period estimated from the separation between A and B (2.6'' or 433 au) and the mass sum is of the order of 3 kyr. The position angle of A,B has increased from 108 $^\circ$ at its discovery in 1825 to 120 $^\circ$ now. Notably, the outer pair has a direct motion, while both inner orbits are retrograde. The short observed arc does not constrain the outer orbit. A notional orbit with a period of 5 kyr is provided as illustration in Figure 4.

3.2. Architecture of FIN 332

FIN 332 is a typical 2+2 quadruple system of ϵ Lyr type (Tokovinin 2008). All four stars have comparable

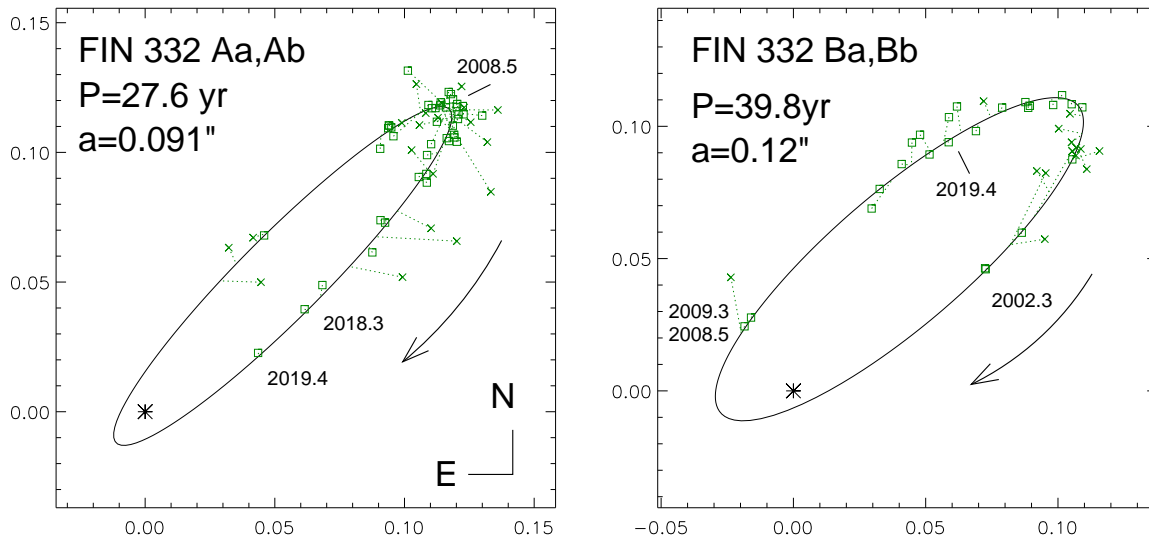


Figure 4. Orbits of inner subsystems Aa,Ab and Ba,Bb in FIN 332.

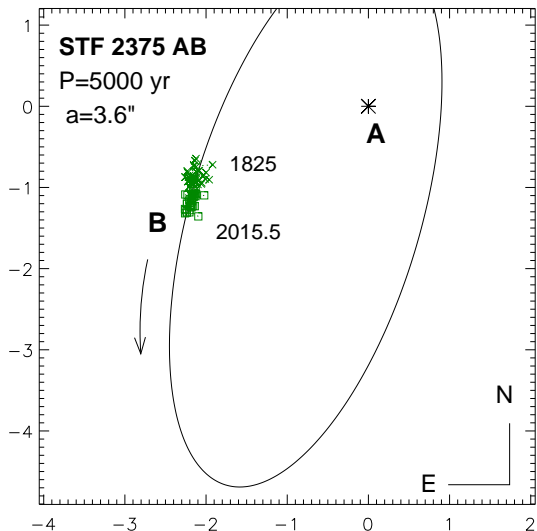


Figure 5. Notional outer orbit of STF 2375 AB. Only a small arc is covered since the discovery of this pair in 1825. The orbital elements are given in Table 1.

masses and luminosities, meaning that they were not chosen randomly from some general mass distribution. Like in many other 2+2 quadruples, the periods of the inner subsystems are comparable. Most remarkably, however, the two inner orbits also have similar orientation in the sky (Figure 4), similarly large eccentricities, and similar orientation of the lines of apsides. Mutual inclination between orbits of Aa,Ab and Ba,Bb is either 16.1° or 141.5° (the orbital nodes are ambiguous).

Relative inclinations of the inner subsystems to the tentative outer orbit are either $56 - 60^\circ$ or $135 - 150^\circ$. These numbers are only indicative, given the uncertain orbit of A,B. However, approximate coplanarity between outer and inner orbits is excluded by the apparent counter-rotation. Large mutual inclination leads to Kozai-Lidov cycles which can drive inner eccentricity to large values. Indeed, both inner orbits are very eccentric.

Components of this system have fast axial rotation of $\sim 150 \text{ km s}^{-1}$ typical of early-type A stars, making de-

termination of spectroscopic orbits unlikely. The average RV is $-19.2 \pm 0.9 \text{ km s}^{-1}$ according to Gontcharov (2006). The PMs measured by Gaia can be distorted by orbital motion in the subsystems. This is less likely for B with equal-brightness components. Its Gaia PM, corrected for the motion in the A,B orbit (B moves relative to A at $(+0.8, -3.2) \text{ mas/yr}$) leads to the center-of-mass PM of $(16.4, 0.6) \text{ mas/yr}$. The mean PM of component A deduced from the Gaia and Hipparcos positions is $(+16.2, +1.6) \text{ mas/yr}$, corresponding to the center-of-mass PM of $(15.8, 0.0) \text{ mas/yr}$. The two estimates of the center-of-mass PM are close to each other. Their average, RV, and dynamical parallax of 6 mas lead to the Galactic velocity of $(U, V, W) = (-18.3, -6.3, -12.4) \text{ km s}^{-1}$. This corresponds to young disk population, but cannot be associated with known kinematic groups.

4. SUMMARY AND DISCUSSION

Discovery by Zasche et al. (2019) of potential resonances between inner binaries in doubly eclipsing systems motivated this work. The accuracy of inner periods in the two hierarchies studied here is sufficient to prove that the period ratios are measurably different from rational numbers: 2.87 ± 0.07 and 1.44 ± 0.02 . However, period ratios in resonant multi-planet systems and doubly eclipsing binaries also differ from exact rational numbers by 1-2%, and differences of this order are expected from theory (Tremaine 2020). Note that Tremaine's analysis of close binaries on circular orbits is not directly applicable to our quadruple systems with eccentric inner orbits.

Notional outer orbits allow us to estimate the ratio of inner and outer semimajor axes that governs the strength of dynamical interaction between inner and outer orbits, $\epsilon = \max(a_1, a_2)/a_3$. This parameter is about 0.08 and 0.03 for GJ 225.1 and FIN 332, respectively. Therefore, interaction between inner and outer orbits is far from being negligible. Dynamical analysis of these systems is beyond the scope of this paper which focuses on assembling the observational data – orbits and masses.

It is instructive to speculate on the formation mechanisms of these hierarchies. Their structure is far from being chaotic: the orbits show some mutual alignment,

and the masses of components in each system are comparable (except GJ 225.1 E). It appears unlikely that these hierarchies experienced strong internal or external (in a cluster) dynamical interactions. Multiple systems surviving chaotic dynamics are different: they have eccentric and misaligned orbits, while their masses are not so well correlated (Sterzik & Tokovinin 2002).

Similar masses imply that components of these hierarchies accreted gas from a common source. Most likely, these systems formed in relative isolation by collapse of an overdensity (core or filament). This scenario was proposed as formation mechanism of wide hierarchies composed of similar solar-type stars (Tokovinin 2020); their wide outer separations imply absence of close neighboring stars. Recent hydrodynamical simulations of isolated cloud collapse show successive formation of protostars, migration of binaries to shorter periods driven by accretion, and formation of outer companions that, in turn, accrete and migrate inward (Lee et al. 2019; Kuffmeier et al. 2019).

Accretion-driven migration is a viable mechanism to form close (spectroscopic) binaries (Tokovinin & Moe 2020). In this respect, it is important to note that some 2+2 hierarchies contain inner close subsystems. For example, the wide 2+2 hierarchy ADS 9716 (HIP 76563/76566, outer projected separation 1.6 kau) contains inner spectroscopic subsystems with periods of 3.3 and 14.3 days and counts six stars in total (Tokovinin 1998). Presence of close inner binaries is a strong (albeit indirect) argument for accretion-driven evolution of stellar hierarchical systems.

Successive formation of companions during collapse of an isolated cloud and their inward migration matches the architecture of compact planetary-like hierarchical systems where all orbits are approximately coplanar, their eccentricities are moderate, and the ratios of periods are not extreme, e.g. the 3+1 quadruple HD 91962 (Tokovinin et al. 2015a). This architecture is typical for low-mass hierarchies (Tokovinin 2018). It matches the properties of GJ 225.1, except that this is a 2+2 hierarchy. The low-mass companion E could be formed by disk fragmentation; a massive and unstable disk around C could be produced by a late accretion burst, when most of the mass has already been accreted by the first three stars A, B, and C. This scenario explains the low mass ratio of C,E. It could work for other hierarchies containing inner subsystems with low mass ratios, e.g. α Gem (HIP 36850), a visual pair where each star is a single-lined spectroscopic binary.

The architecture of the more massive quadruple system FIN 332 (the Tweedles) is different: its inner and outer orbits are definitely misaligned, although the inner orbits might still be mutually aligned. Statistically, there is no alignment between inner orbits of resolved 2+2 quadruple systems, as can be inferred from the comparable numbers of apparently co- and counter-rotating inner pairs. In this sense, FIN 332 is atypical. Similarity of orientation and eccentricities of its inner orbits is truly remarkable. Hypothetically, such quadruples re-

sembling ϵ Lyr could form by the outside-in hierarchical collapse, possibly triggered by collision (Whitworth 2001). However, the similarity of component's masses in such quadruples still suggests accretion from a common source. Accretion helps to shrink the initially wide (on the order of Jeans length?) stellar hierarchies to their actual size. Overall, larger and more massive hierarchies are less aligned in comparison to their smaller and less massive counterparts (Tokovinin 2017).

The two hierarchical systems presented here could be studied in detail owing to the happy coincidence of their parameters (separations, mass ratios, distance) with past and current observational capabilities and the existence of adequate time coverage. Continued monitoring of other hierarchical systems and data from large surveys will provide material for study of their dynamics and origin.

The work of Tokovinin is supported by NOIRlab, which is managed by Association of Universities for Research in Astronomy (AURA) under a cooperative agreement with the National Science Foundation.

REFERENCES

- Baize, P. 1980, *Inf. Circ. IAU Comm.* 26, 80, 1
- Balega, I. I., Balega, Yu. Yu., Gasanova, L. T., et al. 2013, *Astrophys. Bull.* 68, 53
- Bressan, A., Marigo, P., Girardi, L., et al. 2012, *MNRAS*, 427, 127
- Gaia Collaboration, Brown, A. G. A., Vallenari, A., Prusti, T., et al. 2018, *A&A*, 595, 2 (Vizier Catalog I/345/gaia2).
- Gontcharov, G. A. 2006, *AstL*, 32, 759
- Kuffmeier, M., Calcutt, H., & Kirstensen, L.. E. 2019, *A&A*, 628, 112
- Lee, A. T., Offner, S., Kratter, K. et al. 2019, *ApJ*, 887, 232
- Mardling, R. A. & Aarseth, S. J. 2002, *MNRAS*, 321, 398
- Mason, B. D., Wycoff, G. L., Hartkopf, W. I., Douglass, G. G. & Worley, C. E. 2001, *AJ*, 122, 3466
- Mason, B. D. 2018, *Inf. Circ.* 196, 3
- Mason, B. D., Hartkopf, W. I., & McAlister, H. A. 2010, *AJ* 140, 242
- Naoz, S. 2016, *ARAA*, 54, 441
- Sterzik, M. & Tokovinin, A. 2002, *A&A*, 384, 1030
- Tokovinin, A. 1982, *AstL*, 8, 99
- Tokovinin, A. 1998, *AstL*, 24, 795
- Tokovinin, A., Kiyaveva, O., Sterzik, M., et al. 2005, *A&A*, 441, 695
- Tokovinin, A. 2008, *MNRAS*, 389, 925
- Tokovinin, A. 2014, *AJ*, 147, 87
- Tokovinin, A., Pribulla, T., & Fischer, D. 2015b, *AJ*, 149, 8
- Tokovinin, A., Latham, D. W., & Mason, B. D. 2015a, *AJ*, 149, 195
- Tokovinin, A. 2016, *ORBIT: IDL Software for Visual, Spectroscopic, and Combined Orbits*, Zenodo, doi:10.2581/zenodo.61119
- Tokovinin, A. 2017, *ApJ*, 844, 103
- Tokovinin, A. 2018, *AJ*, 155, 160
- Tokovinin, A., Mason, B. D., Mendez, R. A. et al. 2020, *AJ*, 160, 7
- Tokovinin, A. 2020, *AJ*, 159, 265
- Tokovinin, A. & Moe, M. 2020, *MNRAS*, 491, 5158
- Tremaine, S. 2020, *MNRAS*, 493, 5583
- Whitworth, A. P. 2001, in: *Proc. IAU Symp.* 200, eds. H. Zinnecker & R. D. Mathieu (ASP: San Francisco)
- Zasche, P., Vokrouhlický, D., Wolf, M., et al. 2019, *A&A*, 630, 128